Antitumor Complexes

DOI: 10.1002/anie.201407406

Platinum(II)–Gadolinium(III) Complexes as Potential Single-Molecular Theranostic Agents for Cancer Treatment**

Zhenzhu Zhu, Xiaoyong Wang, Tuanjie Li, Silvio Aime, Peter J. Sadler, and Zijian Guo**

Abstract: *Theranostic agents are emerging multifunctional molecules capable of simultaneous therapy and diagnosis of diseases. We found that platinum(II)–gadolinium(III) complexes with the formula $[\{Pt(NH_3)_2Cl\}_2GdL](NO_3)_2$ possess such properties. The Gd center is stable in solution and the cytoplasm, whereas the Pt centers undergo ligand substitution in cancer cells. The Pt units interact with DNA and significantly promote the cellular uptake of Gd complexes. The cytotoxicity of the Pt–Gd complexes is comparable to that of cisplatin at high concentrations (≥ 0.1 mM), and their proton relaxivity is higher than that of the commercial magnetic resonance imaging (MRI) contrast agent Gd–DTPA. T_1-weighted MRI on B6 mice demonstrated that these complexes can reveal the accumulation of platinum drugs in vivo. Their cytotoxicity and imaging capabilities make the Pt–Gd complexes promising theranostic agents for cancer treatment.*

Platinum anticancer drugs, such as cisplatin, have been widely used to treat various cancers for nearly 40 years.[1] However, novel Pt complexes still attract much attention because resistance and severe side effects are frequently observed with existing Pt drugs.[2] The cationic Pt^{II} complex *cis*-$[Pt(NH_3)_2(py)Cl]^+$ (py is a pyridyl ligand), for example, displayed significant anticancer activity in murine tumor models and showed promise for overcoming drug resistance.[3] Regrettably, the behavior of these complexes, such as distribution, accumulation, and metabolism, in tumors is poorly understood. Thus, a reliable strategy for real-time monitoring of the drug location and therapeutic responses during treatment is highly desired. Direct information on drug action would provide the basis for minimizing the duration of ineffective courses of treatment and for adopting a personalized therapeutic regimen in cancer therapy.[4]

Multifunctional Pt complexes are likely to exhibit synergic actions against tumor cells.[5] Commonly, they can enhance selectivity for cancer cells or modulate the drug distribution in the body to increase drug accumulation at tumor sites.[1,6] Furthermore, by the conjugation of Pt pharmacophores to fluorescent groups, these complexes could be developed as theranostic agents with both therapeutic and diagnostic capabilities.[7] Nevertheless, since these functions rely on drug release and fluorescence changes induced by tumor-associated stimuli, the fluorescence intensity may not correlate well with the actual drug concentration if the release is incomplete or blocked; besides, no direct information can be obtained on the therapeutic efficacy.

MRI provides a powerful noninvasive diagnostic modality for cancers with high spatial resolution (10–100 μm) and precise 3D positioning.[8] We recently showed that Pt drugs could be attached to Fe_2O_3 nanoparticles to form anticancer theranostic agents, in which nanoparticles act as both drug carriers and T_2-weighted MRI contrast agents (CAs).[9] However, release procedures are indispensable for these nanomedicines. As alternatives, Gd^{III} complexes are widely used as T_1-weighted CAs in MRI through the interaction of inner-sphere water with paramagnetic Gd^{III} and rapid exchange of the coordinated water with the bulk solvent.[10] For example, gadolinium diethylenetriaminepentaacetate ($[Gd(DTPA)(H_2O)]^{2-}$, Gd–DTPA, or Magnevist) is one of the most common MRI CAs in the clinic because of its low toxicity, rapid renal clearance, and high stability.[11] Some polymeric micelles derived from the self-assembly of Gd–DTPA, Pt pharmacophores, and block copolymers, such as PEG-*b*-P(Glu) and PEG-*b*-PAsp(DET), have been developed as theranostic agents.[12] Interestingly, a Pt–Gd complex containing Gd–DTPA and $\{Pt^{II}$(2,2′:6′,2″-terpyridine)$\}$ units was shown to selectively accumulate in the nuclei of tumor cells.[13]

We herein report two Pt–Gd complexes, **1** and **2**, as cancer theranostic agents (Scheme 1). Multidentate ligands **L1** and **L2** were obtained by modifying DTPA with pyridin-2-ylmethanamine and pyridin-2-ylethanamine, respectively; **1** and **2** were formed by conjugating **GdL1** and **GdL2** to the cytotoxic *cis*-$[Pt(NH_3)_2Cl]^+$ complex, respectively. Thus, the Gd–DTPA and Pt complexes were integrated into a single molecule with both anticancer and imaging functionalities. These complexes can enter cancer cells and interact with DNA; more importantly, they show higher proton relaxivity

[*] Z. Zhu, Dr. T. Li, Prof. Dr. Z. Guo
State Key Laboratory of Coordination Chemistry
School of Chemistry and Chemical Engineering
Nanjing University, Nanjing 210093 (P. R. China)
E-mail: zguo@nju.edu.cn
Prof. Dr. X. Wang
State Key Laboratory of Pharmaceutical Biotechnology, School of Life Sciences; State Key Laboratory of Analytical Chemistry for Life Science, Nanjing University, Nanjing 210093 (P.R. China)
E-mail: boxwxy@nju.edu.cn
Prof. Dr. S. Aime
Center of Molecular Biotechnology, University of Torino
Via Nizza, 52, 10126 Torino (Italy)
Prof. Dr. P. J. Sadler
Department of Chemistry, University of Warwick
Gibbet Hill, Coventry, CV4 7AL (UK)

[**] We appreciate the financial support from the National Natural Science Foundation of China (No. 21271101, 21131003, 21021062, 91213305), the National Basic Research Program of China (2011CB935800), and the ERC (No. 247450). We also thank Dr. Rebecca Steele and Dr. Gianni Ferrante of Stellar for the NMRD measurement.

Supporting information for this article is available on the WWW under http://dx.doi.org/10.1002/anie.201407406.

 © 2014 Wiley-VCH Verlag GmbH & Co. KGaA, Weinheim

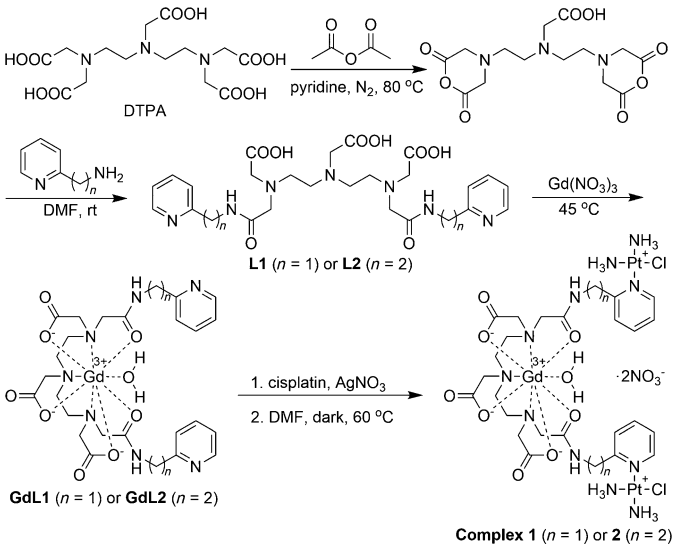

Scheme 1. Synthetic route to Pt–Gd complexes **1** and **2**.

than that of Gd–DTPA and similar cytotoxicity to that of cisplatin at imaging concentrations. Therefore, they are capable of simultaneous drug tracing and cancer restraint.

The formation of **1** and **2** was confirmed by ESIMS (see Figure S1 and Table S1 in the Supporting Information). The complex cations and related species indicate that the skeleton of **1** and **2** is stable and the chlorides are dissociable in aqueous solution. Moreover, the inner-sphere water is exchangeable, which is essential for CAs to increase the relaxation rate of the bulk solvent.[10] It is known that intracellular glutathione (GSH) tends to react with Pt complexes and promote leaving of the opposite ligand as a result of the *trans*-labilization effect.[14] The stability of **2** in the presence of GSH was thus examined by ESIMS (see Figure S2 and Table S2). The results showed that the Pt moieties could leave the complex in this situation. However, the complex ion at m/z 642.42 remained the major species even at 48 h, thus showing that the release of Pt moieties is a slow and incomplete process. The limited dissociation may lower the cytotoxicity of the Pt unit(s) towards cancer cells and enable the Pt–Gd complex to act as an MRI CA at a relatively high concentration.

The interactions of complexes **1** and **GdL1** with DNA were first studied by circular dichroism (CD). Figure 1 A displays CD spectra of calf-thymus DNA (CT-DNA) in the presence of **1**. The dramatic decrease in ellipticity for both positive and negative bands suggests that **1** can unwind the DNA helix and lead to the loss of helicity through rotation of the bases.[15] However, **GdL1** only induced a slight change in ellipticity (see Figure S3), thus suggesting that it affects DNA mainly through electrostatic interactions.[16] Since the CD change induced by cisplatin is a slight increase in ellipticity of the positive band,[17] the DNA-binding mode of **1** appears to be different from that of cisplatin. The interactions were further studied by using supercoiled pUC19 plasmid DNA electrophoresis in a native agarose gel. It is known that the binding of unwinding agents to closed circular DNA can reduce its superhelical density and hence decrease the DNA migration rate in agarose gel.[18] Complex **1** caused a conspicuous decrease in the mobility of DNA (Figure 1 B), whereas **GdL1** induced no significant changes in the migration of DNA (see Figure S3), thus indicating that only **1** can unwind the DNA superhelix. Similar results were also observed for **2** and **GdL2** under the same conditions (see Figure S4). The results confirm that **1** and **2** can significantly interfere with the helicity of DNA, and that the interference is primarily induced by the Pt moieties. If these complexes can enter cancer cells, such interference may lead to distortions in nuclear DNA and result in cell death.[1]

The cellular uptake of **GdL1**, **GdL2**, **1**, and **2** in HeLa cells was determined by ICPMS after the cells were exposed to each complex for 24 h. The content of Gd and Pt in the cytoplasm and nucleoplasm is listed in Table 1. The results indicate that all the complexes can enter the cells and accumulate in the cytoplasm, but only **1** and **2** can travel further into the nuclei. The molar ratios of Pt to Gd for **1** and **2** did not match with their stoichiometric ratio, as it was less than 2:1 in the cytoplasm (0.35 and 0.34, respectively) but larger than 2:1 in the nucleoplasm (13.89 and 2.40, respectively). This observation suggests that **1** and

Table 1: Cellular uptake of Gd and Pt after the incubation of 10^6 HeLa cells with **GdL1**, **GdL2** (100 μM), **1**, and **2** (40 μM) for 24 h. Data are expressed as the mean (μM) ± standard deviation of at least three independent experiments, with untreated cells as the control.

Complex	Cytoplasm[a]		Nucleoplasm[a]	
	Gd	Pt	Gd	Pt
GdL1	540.3 ± 10.0	–	–	–
GdL2	541.5 ± 4.9	–	–	–
1	668.7 ± 38.9	233.8 ± 15.2	15.6 ± 3.2	216.7 ± 10.2
2	862.4 ± 10.3	290.8 ± 16.0	44.5 ± 5.6	107.0 ± 2.4

[a] The control value has been subtracted.

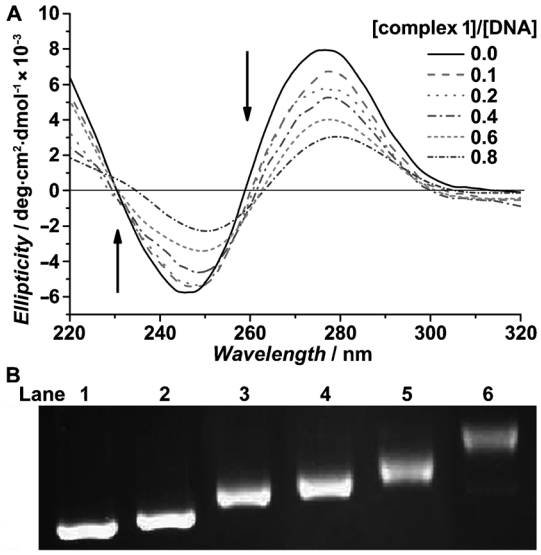

Figure 1. A) CD spectra of CT-DNA (1.0×10^{-4} M) in the presence of **1** at different [**1**]/[CT-DNA] molar ratios, and B) agarose-gel electrophoresis patterns of supercoiled pUC19 plasmid DNA (200 ng) after incubation with **1** in a buffer (50 mM Tris–HCl, 50 mM NaCl, pH 7.4; Tris = 2-amino-2-hydroxymethylpropane-1,3-diol) at 37 °C for 12 h. Lane 1: DNA control, lanes 2–6: DNA + **1** (20, 40, 60, 80, 100 μM, respectively).

© 2014 Wiley-VCH Verlag GmbH & Co. KGaA, Weinheim

2 partially dissociated in the cells, and that the released Pt moieties effused from the cells or entered the nuclei more readily than the Gd complexes. Interestingly, the Gd content for **1** and **2** was apparently higher than that for **GdL1** and **GdL2** in the cytoplasm, although the incubation concentration of **1** and **2** (40 μM) was much lower than that of **GdL1** and **GdL2** (100 μM). This result suggests that the Pt units facilitate the cellular uptake of the Gd complexes. Most gadolinium-based CAs, including Gd–DTPA, are restricted to extracellular spaces and lack the ability to accumulate within cells.[19] Herein we demonstrate that Gd–DTPA can be transformed into a membrane-permeable intracellular CA by linking aryl amine groups to the ligand, possibly by the minimization of osmolality owing to their nonionic nature. To our surprise, conjugation with *cis*-$[Pt(NH_3)_2Cl]^+$ further improved the membrane permeability of the Gd complexes. In view of their remarkable cellular uptake and appropriate dissociation tendency (see above), these Pt–Gd complexes have the potential to produce detectable MRI signals and cytotoxic activity in cancer cells.

The cytotoxicity of **1** and **2** against the human breast cancer MCF-7, the human non-small-cell lung cancer A549, and the human cervical cancer HeLa cell lines are summarized in Table 2 (see also Figure S5). Cisplatin was used as the control. The inhibition efficacy of **1** and **2** is lower than that of cisplatin towards these cell lines, particularly at low concentrations (1–50 μM). However, they exhibit similar efficacy to that of cisplatin at a higher concentration of 0.1 mM (see Figure S6). Such a concentration is sufficient for gadolinium-based CAs to produce an effective contrast effect. Excessive cytotoxicity would destroy the cells before the imaging concentration was reached. Thus, **1** and **2** can fulfil the cytostatic and imaging functions simultaneously within the same dose. As expected, **GdL1** and **GdL2**, or the residual parts of **1** and **2** after loss of the Pt moieties, are almost nontoxic towards these cell lines.

Table 2: IC_{50} (μM) values of complexes **1**, **2**, and cisplatin for MCF-7, A-549, and HeLa cancer cell lines at 48 h.

Complex	Cell line		
	MCF-7	A549	HeLa
cisplatin	4.18 ± 0.32	3.89 ± 0.62	6.39 ± 1.05
1	27.22 ± 1.90	21.15 ± 1.68	35.24 ± 1.72
2	27.75 ± 2.53	25.04 ± 3.47	29.67 ± 1.59

Proton nuclear magnetic relaxation dispersion (NMRD) is commonly used to evaluate the efficacy of potential MRI CAs.[20] Proton NMRD profiles of the relaxivity (r_1), which is defined as the longitudinal-relaxation-rate enhancement produced by a Gd complex at a concentration of 1 mM,[21] are shown in Figure 2 A for **GdL1**, **GdL2**, **1**, **2**, and Gd–DTPA. All new complexes demonstrated an increased relaxivity relative to the parent complex Gd–DTPA (4.3 $mM^{-1}s^{-1}$). This increase in relaxivity may be induced by the decreased rotational mobility of the complexes. The high relaxivities of **1** and **2** at 20 MHz (ca. 6.3 $mM^{-1}s^{-1}$) imply that they are potential T_1-weighted MRI CAs for monitoring real-time drug distribution during cancer treatment. This behavior was first verified by in vitro assays. The T_1-weighted MR images for the cell-free

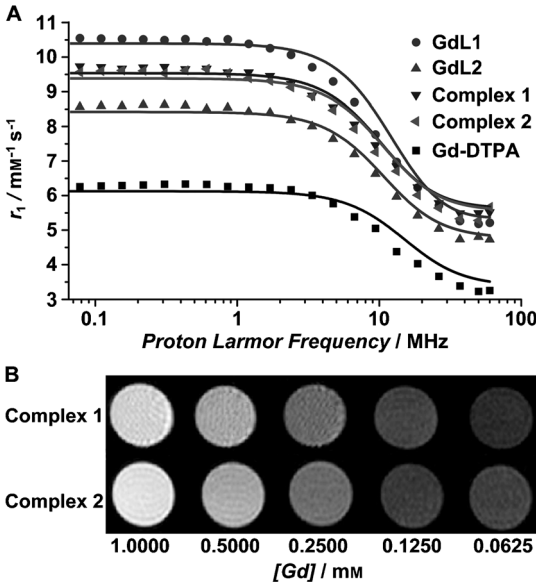

Figure 2. A) NMRD profiles of **GdL1**, **GdL2**, **1**, **2**, and Gd–DTPA (1 mM) at different magnetic-field-strength values at 37 °C, and B) T_1-weighted MR images of **1** and **2** versus the concentration of Gd^{III} at 0.52 T and 37 °C.

solutions of **1** and **2** varied markedly, and the signal intensity was positively correlated with the Gd concentration (Figure 2 B). The minimum detection limit for **1** and **2** was 110 and 62 μM, respectively (see Table S3). Assays of a suspension of HeLa cells treated with **1** or **2** gave similar images; that is, the signal intensity increased significantly as compared with that of the untreated cellular suspension (see Figure S7). Under the same conditions, **1** was somewhat less effective than **2**. This difference seems to be associated with their cellular-uptake profiles (Table 1). The contrast effect decreased with time, thus suggesting that some of the Gd complex was excreted from the cells after releasing the Pt units. The results again confirm that **1** and **2** can enter cancer cells.

In vivo MR images were acquired at various time points after the solutions of **1**, **2**, and Gd–DTPA were injected into B6 mice, respectively. Complexes **1** and **2** induced more evident MR-signal enhancement in the kidneys than Gd–DTPA did under the same conditions (Figure 3). The signal intensity attenuated gradually after 8 min for all complexes; however, in comparison with Gd–DTPA, **1** and **2** can maintain the intensity at relatively high levels for more than 1 h, thereby providing the possibility of renal imaging over an extended period of time. Since cisplatin can cause renal tubular damage or dysfunction,[22] many MRI methods have been developed to detect cisplatin-induced acute renal failure in animal models.[23] However, the imaging of small animals, such as mice, is quite difficult because the need for rapid scanning severely limits the image resolution. The fast accumulation and slow excretion of **1** and **2** in the kidneys may offer an opportunity for the in situ detection of acute renal injury caused by Pt drugs during treatment.

In conclusion, we have developed two bifunctional Pt–Gd complexes as theranostic agents for cancer treatment. These complexes partially dissociate in cancer cells to provide cytostatic Pt moieties, whereas the residual Gd component

 © 2014 Wiley-VCH Verlag GmbH & Co. KGaA, Weinheim

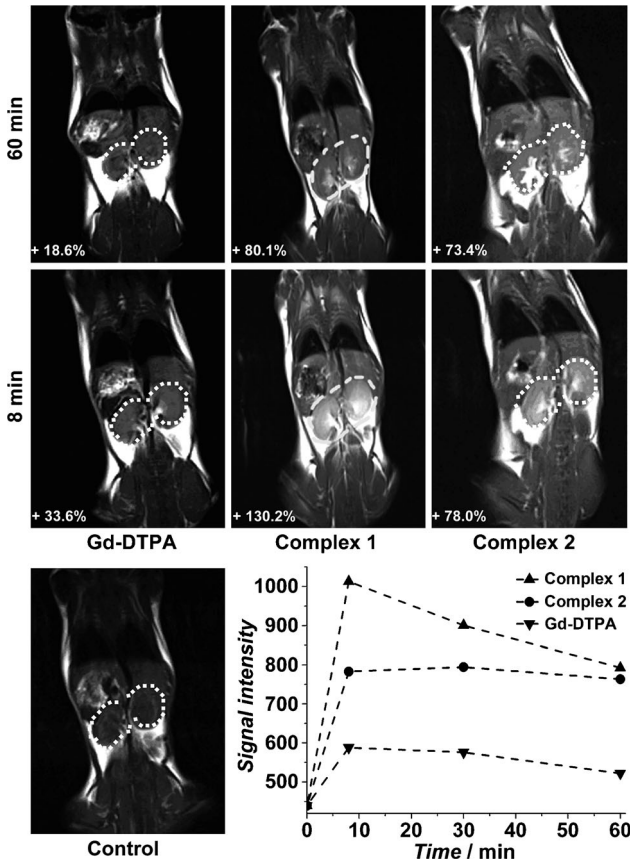

Figure 3. In vivo T_1-weighted MR images of B6 mice at 8 and 60 min after the injection of **1**, **2**, and Gd–DTPA at a dose of 0.1 mmol Gd^{III}/kg of body weight and the corresponding signal-decay curves. The circles indicate the area of the kidneys.

and the untouched complex can be used for imaging. The Pt units can greatly improve the cellular uptake of Gd complexes, and the proton relaxivities of the Pt–Gd complexes are higher than that of Gd–DTPA under physiological conditions. Furthermore, these complexes display the extraordinary trait of biocompatibility: Their relatively low cytotoxicity enables them to satisfy the tumor-imaging and inhibition requirements at the same dose. In particular, these complexes remain longer in the kidneys of mice, which offers the possibility of the noninvasive diagnosis of acute renal injury by nephrotoxic platinum drugs in mice models, or probably, after further development, in patients.[23] In a more general sense, these membrane-permeable complexes may be used to monitor the temporal distribution of Pt drugs in vivo, to directly assess the therapeutic response in situ, or to obtain diagnostic images for preventing irreversible damage to patients.

Received: August 1, 2014
Published online: September 26, 2014

Keywords: antitumor agents · gadolinium · imaging agents · platinum · theranostic agents

[1] X. Y. Wang, Z. J. Guo in *Bioinorganic Medicinal Chemistry* (Ed.: E. Alessio), Wiley-VCH, Weinheim, **2011**, pp. 97 – 149.
[2] a) N. J. Farrer, J. A. Woods, L. Salassa, Y. Zhao, K. S. Robinson, G. Clarkson, F. S. Mackay, P. J. Sadler, *Angew. Chem. Int. Ed.* **2010**, *49*, 8905 – 8908; *Angew. Chem.* **2010**, *122*, 9089 – 9092; b) Đ. U. Miodragović, J. A. Quentzel, J. W. Kurutz, C. L. Stern, R. W. Ahn, I. Kandela, A. Mazar, T. V. O'Halloran, *Angew. Chem. Int. Ed.* **2013**, *52*, 10749 – 10752; *Angew. Chem.* **2013**, *125*, 10949 – 10952.
[3] a) K. S. Lovejoy, R. C. Todd, S. Zhang, M. S. McCormick, J. A. D'Aquino, J. T. Reardon, A. Sancar, K. M. Giacomini, S. J. Lippard, *Proc. Natl. Acad. Sci. USA* **2008**, *105*, 8902 – 8907; b) D. Wang, G. Zhu, X. Huang, S. J. Lippard, *Proc. Natl. Acad. Sci. USA* **2010**, *107*, 9584 – 9589.
[4] T. Lammers, S. Aime, W. E. Hennink, G. Storm, F. Kiessling, *Acc. Chem. Res.* **2011**, *44*, 1029 – 1038.
[5] a) D. Griffith, M. P. Morgan, C. J. Marmion, *Chem. Commun.* **2009**, 6735 – 6737; b) Z. Q. Xue, M. X. Lin, J. H. Zhu, J. F. Zhang, Y. Z. Li, Z. J. Guo, *Chem. Commun.* **2010**, *46*, 1212 – 1214.
[6] S. Ding, X. Qiao, G. L. Kucera, U. Bierbach, *J. Med. Chem.* **2012**, *55*, 10198 – 10203.
[7] a) Y. Yuan, R. T. K. Kwok, B. Z. Tang, B. Liu, *J. Am. Chem. Soc.* **2014**, *136*, 2546 – 2554; b) S. D. Wu, X. Y. Wang, C. C. Zhu, Y. J. Song, J. Wang, Y. Z. Li, Z. J. Guo, *Dalton Trans.* **2011**, *40*, 10376 – 10382.
[8] R. Weissleder, M. J. Pittet, *Nature* **2008**, *452*, 580 – 589.
[9] J. Z. Wang, X. Y. Wang, Y. J. Song, J. Wang, C. L. Zhang, C. J. Chang, J. Yan, L. Qiu, M. M. Wu, Z. J. Guo, *Chem. Sci.* **2013**, *4*, 2605 – 2612.
[10] P. Caravan, *Chem. Soc. Rev.* **2006**, *35*, 512 – 523.
[11] S. Laurent, C. Henoumont, L. Vander Elst, R. N. Muller, *Eur. J. Inorg. Chem.* **2012**, 1889 – 1915.
[12] a) S. Kaida, H. Cabral, M. Kumagai, A. Kishimura, Y. Terada, M. Sekino, I. Aoki, N. Nishiyama, T. Tani, K. Kataoka, *Cancer Res.* **2010**, *70*, 7031 – 7041; b) P. Mi, H. Cabral, D. Kokuryo, M. Rafi, Y. Terada, I. Aoki, T. Saga, I. Takehiko, N. Nishiyama, K. Kataoka, *Biomaterials* **2013**, *34*, 492 – 500.
[13] E. L. Crossley, J. B. Aitken, S. Vogt, H. H. Harris, L. M. Rendina, *Angew. Chem. Int. Ed.* **2010**, *49*, 1231 – 1233; *Angew. Chem.* **2010**, *122*, 1253 – 1255.
[14] M. E. Oehlsen, Y. Qu, N. Farrell, *Inorg. Chem.* **2003**, *42*, 5498 – 5506.
[15] a) W. C. Johnson in *Circular Dichroism: Principles and Applications* (Eds.: K. Nakanishi, N. Berova, R. W. Woody), VCH, New York, **1994**, pp. 523 – 540; b) K. Karidi, A. Garoufis, N. Hadjiliadis, J. Reedijk, *Dalton Trans.* **2005**, 728 – 734.
[16] S. P. Tang, L. Hou, Z. W. Mao, L. N. Ji, *Polyhedron* **2009**, *28*, 586 – 592.
[17] M. Gay, Á. M. Montaña, V. Moreno, M. J. Prieto, R. Llorens, L. Ferrer, *J. Inorg. Biochem.* **2005**, *99*, 2387 – 2394.
[18] M. V. Keck, S. J. Lippard, *J. Am. Chem. Soc.* **1992**, *114*, 3386 – 3390.
[19] P. Caravan in *Molecular and Cellular MR Imaging* (Eds.: M. M. J. Modo, J. W. M. Bulte), CRC, Boca Raton, FL, **2007**. pp. 13 – 36.
[20] P. Caravan, J. J. Ellison, T. J. McMurry, R. B. Lauffer, *Chem. Rev.* **1999**, *99*, 2293 – 2352.
[21] K. Kimpe, T. N. Parac-Vogt, S. Laurent, C. Piérart, L. Vander Elst, R. N. Muller, K. Binnemans, *Eur. J. Inorg. Chem.* **2003**, 3021 – 3027.
[22] H. Zhou, T. Miyaji, A. Kato, Y. Fujigaki, K. Sano, A. Hishida, *J. Lab. Clin. Med.* **1999**, *134*, 649 – 658.
[23] H. Kobayashi, S. Kawamoto, S. K. Jo, N. Sato, T. Saga, A. Hiraga, J. Konishi, S. Hu, K. Togashi, M. W. Brechbiel, R. A. Star, *Kidney Int.* **2002**, *61*, 1980 – 1985.

 © 2014 Wiley-VCH Verlag GmbH & Co. KGaA, Weinheim